Available online at www.sciencedirect.com
SCIENCE DIRECT®
Cement and Concrete Research 33 (2003) 881–890
CEMENT AND CONCRETE RESEARCH

Shape and "gap" effects on the behavior of variably confined concrete

Kent A. Harries*, Shawn A. Carey

Department of Civil and Environmental Engineering, University of South Carolina, 300 Main Street, Columbia, SC 29208, USA

Received 11 July 2002; accepted 10 December 2002

Abstract

Factors affecting the behavior of variably confined concrete are presented. The effect of debonding the fiber-reinforced polymer (FRP) jacket to the concrete substrate and providing a gap between the concrete and confining jacket is investigated. A second parameter—the shape of the cross section—is also investigated. An experimental program involving the compression testing of standard cylinders and similarly sized square specimens having external FRP jackets providing passive confinement is presented. Factors affecting jacket efficiency and the appropriateness of factors accounting for specimen shape are determined experimentally and discussed.

The provision of a gap affected the axial stress at which the confining jacket was engaged, resulting in a reduced maximum attainable concrete strength. The jacket efficiency was not affected by the provision of the gap. The shape of the specimens was observed to affect the level of confinement generated. Square specimens exhibit lower confinement levels than circular specimens having the same jacket.

Keywords: Compressive strength; Expansion; Mechanical properties; Modeling; Nominated, confinement

1. Introduction

The axial stress–strain behaviors of unconfined and confined concrete differ significantly. Furthermore, the nature of the confinement provided also significantly affects the concrete behavior. In conventionally reinforced and externally jacketed concrete columns, confining pressure is *passive* in nature. That is, confining pressure is engaged by the transverse dilation of concrete resulting from principal axial strains—the Poisson effect.

Passive confinement may be *constant* or *variable* through an axial load history. Constant confining pressure is generated in cases where the confining material behaves in a plastic manner. This is typically assumed the case where confinement is provided by conventional transverse reinforcing steel. Variable confining pressure is generated when the confining material has an appreciable stiffness. Fiber-reinforced polymer (FRP) jackets and transverse steel that is still elastic generate variable confining pressures. Variable passive confinement is dependent on the axial and transverse behavior of the concrete, which, in turn, is dependent on the amount and stiffness of confinement provided.

In a companion investigation [1], the experimentally observed axial load behavior of variably confined cylinders having fully bonded FRP composite jackets providing the confinement is reported. In particular, this companion study investigated the relationship between transverse and longitudinal strains—the dilation relationship—and a model for this behavior, based on the stiffness of the confining materials, is proposed.

The objective of the present study is to refine the understanding of factors affecting the behavior of confined concrete identified previously [1]. In this study, the effect of bonding the FRP jacket to the concrete substrate is investigated. It is proposed that an unbonded FRP jacket is analogous to the "slackness" observed in bonded woven FRP jackets [1]. A second parameter—the shape of the cross section—is also investigated. It is recognized that, unlike circular sections, rectilinear sections having external confinement do not experience uniform confining pressure from external confinement. Dilation of the concrete section results in significant confining pressure developed across the diagonals of rectilinear sections. The jacket sides provide smaller levels of confinement since confining pressure at this location is engaged more by the flexural stiffness of

* Corresponding author. Tel.: +1-803-777-0671; fax: +1-803-777-0670.
E-mail address: harries@sc.edu (K.A. Harries).

0008-8846/03/$ – see front matter © 2003 Elsevier Science Ltd. All rights reserved.
doi:10.1016/S0008-8846(02)01085-2

the jacket. In this study, circular and square specimens are tested and compared. Additionally, the square specimens have their corners rounded to two different radii in an effort to experimentally validate existing shape effect modification factors.

An experimental program is presented to investigate the parameters above. The experimental program involves the compression testing of standard cylinders and similarly sized square specimens having external FRP jackets providing passive confinement. This research will increase knowledge of the behavior of confined concrete and help in further developing an existing variably confined concrete model [2].

2. FRP jacket efficiency

Passive confining pressure is engaged by dilation of axially loaded concrete. The confining pressure that may be generated is therefore limited by the material properties of the confining material. External FRP jackets, although very strong and stiff, have relatively small strain capacity. Typically, rupture strains will govern jacket design.

Kestner et al. [3] and Demers [4] report that measured in situ jacket strains at failure are significantly lower than the rupture strains reported by the manufacturer or observed in tensile coupon tests. In both studies, the FRP jackets were fabricated from unidirectional E-glass fabrics. Kestner et al. [3] report maximum in situ jacket strains on 508-mm-diameter reinforced concrete column specimens ranging from 45% to 60% of the experimentally determined material rupture strain. Kestner et al. [3] report slightly larger values of material rupture strain observed on smaller 152-mm-diameter plain concrete cylinders. Demers [4] reports maximum in situ jacket strains on 305-mm-diameter reinforced concrete columns ranging from 33% to 63% of the manufacturer's reported material rupture strain. This apparent in situ jacket inefficiency results in earlier rupture of the jacket and thus lower ultimate confining pressure than may be expected based on reported material properties.

Kharel [5] reported in situ rupture strains of between 69% and 80% of the experimentally determined FRP rupture strain of 0.015. It is noted that Kharel used very lightweight E-glass and carbon FRP materials to provide confinement to 152-mm-diameter standard concrete cylinders [1]. The materials used by Kharel are the same as those used in this study.

Two factors contribute to the observed strain inefficiency [3,6]: a *strain efficiency factor*, which accounts for discrepancies between jacket material properties and those that can be realized in situ, and a *shape factor*, which is dependent on the geometry of the confined concrete section.

2.1. Strain efficiency factor, κ_ε

Pessiki et al. [6] propose a strain efficiency factor, κ_ε, to account for the observed difference between in situ jacket rupture strains and FRP material rupture strains determined from standard coupon tests (typically ASTM D3039 [7]). The strain efficiency factor is the product of two components, $\kappa_{\varepsilon 1}$ and $\kappa_{\varepsilon 2}$. The strain localization factor, $\kappa_{\varepsilon 1}$, is the ratio of the average strain in a jacket around its perimeter to the in situ jacket rupture strain. The in situ properties factor, $\kappa_{\varepsilon 2}$, is the ratio of the in situ jacket rupture strain to the reported or measured material strain capacity, ε_{fr}. The interrelation of these factors may be described by considering the two bounding cases, where either $\kappa_{\varepsilon 1}$ or $\kappa_{\varepsilon 2}$ is equal to unity.

Fig. 1(a) illustrates the case where $\kappa_\varepsilon = \kappa_{\varepsilon 2}$ (that is, $\kappa_{\varepsilon 1} = 1.0$). In this case, no shear may be transferred between the jacket and the concrete, resulting in a uniform distribution of strain in the jacket around the entire perimeter of

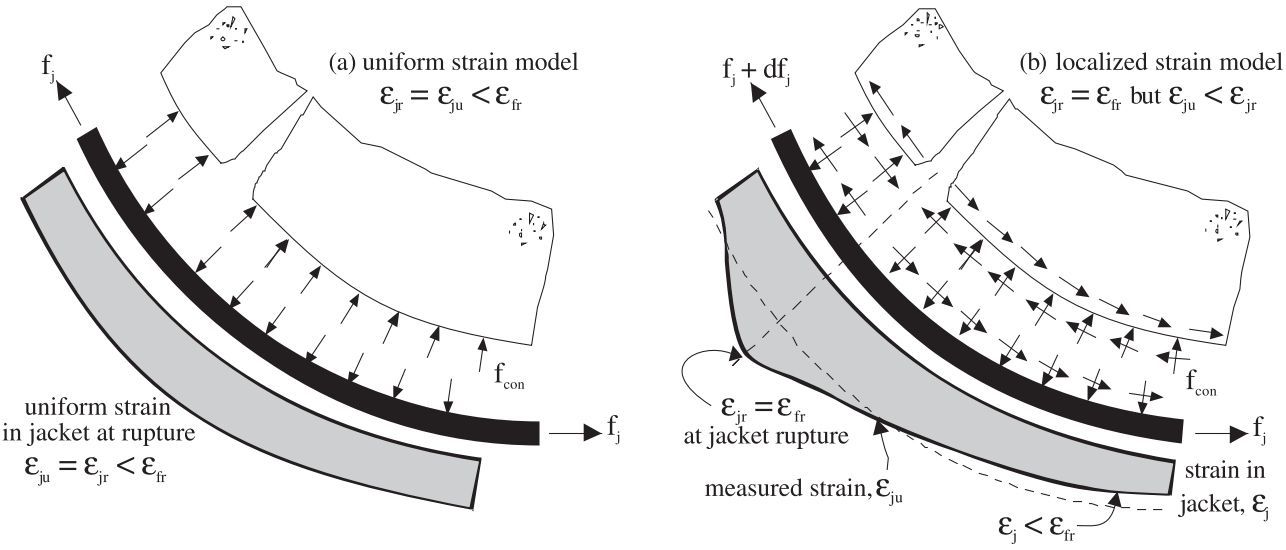

Fig. 1. Schematic representations of uniform and localized strain models [6].

the confined concrete. The discrepancies between in situ strain capacities and material strain capacities accounted for in this manner may include [3,6]:

1. misalignment or damage to jacket fibers during handling and lay-up;
2. the inclusion of residual strains during lay-up resulting from flaws in the substrate concrete, uneven tension during lay-up, or temperature, creep, and shrinkage incompatibility between the concrete and FRP jacket; and,
3. the cumulative probability of weaknesses in FRP material since jackets are much larger than tensile coupons.

The in situ properties factor, $\kappa_{\varepsilon 2}$, may also be used to account for an initial "gap" between the concrete substrate and the FRP jacket. This gap may be real or may result from the "unkinking" or "slackness" of woven FRP materials subject to initial tension as described in the companion paper [1].

The model for localized strain, where $\kappa_{\varepsilon} = \kappa_{\varepsilon 1}$ (that is, $\kappa_{\varepsilon 2} = 1.0$), is shown in Fig. 1(b). In this case, localized regions of high strain occur in the jacket (in the case illustrated in Fig. 1, bridging a splitting crack). The bond between the jacket and underlying concrete allows concentrated jacket stresses to be transferred into the concrete away from the crack and thus reduces the average strain in the jacket. A profile of the supposed strain distribution, ε_j, in the jacket material is shown in Fig. 1(b). This figure illustrates why, unless a measurement is made exactly at the strain concentration, measured jacket strains at rupture, ε_{ju}, are lower than the material strain capacity, ε_{fr}, which is only reached at the stress concentration.

The actual strain efficiency is a combination of the strain localization and in situ strain efficiency factors. Further investigation is required to identify all of the parameters that contribute to the relative proportioning of these factors [6].

The variability of attainable in situ jacket strains results in a similar variability in attainable confining pressure and therefore concrete behavior. In addition, it is not only FRP strain at rupture that appears to have reduced values in situ, considerable variance in FRP material stiffness, and thus capacity, was observed by Kestner et al. [3]. It is believed that this variability is mostly a function of the differences in lay-up technique between in situ and tensile coupon applications. It has been found, however, that for most external confinement applications, strain capacity of the jacket is the dominant design criteria.

2.2. Shape factor

FRP jackets have very high in-plane tensile stiffness but, as they are typically quite thin, very small out-of-plane flexural stiffness. Effective confining pressure is therefore only generated where the jacket is engaged in tension. The entire cross section of a circular column having external confinement is influenced by the confining force generated by hoop stress in the confinement. Rectangular columns, on the other hand, do not experience uniform confining pressure from external confinement. Dilation of the concrete section results in large confining pressures developed across the diagonals of rectangular sections. The jacket sides provide smaller levels of confinement since confining pressure at this location is engaged more by the flexural stiffness of the thin jacket rather than the tensile stiffness of the jacket as shown schematically in Fig. 2.

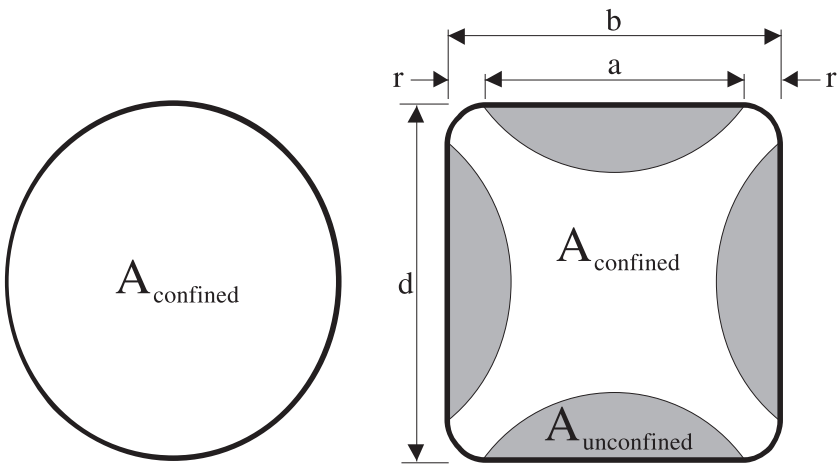

(a) confined region for a circular section

(b) confined region for a rectangular section

Fig. 2. Geometry of confined region of core concrete.

Restrepol and DeVino [8] have proposed a definition of the confined core concrete for square (or rectangular) columns confined with external jackets. This definition provides for an arc-shaped region of unconfined material along the sides of a square or rectangular column as shown in Fig. 2(b). This definition is analogous to the assumed confinement provided by rectilinear column ties [9]. Based on this definition, an effective area of confined concrete, A_{confined}, may be determined:

$$A_{\text{confined}} = A_g\left[1 - \left[\frac{(b-2r)^2 + (d-2r)^2}{3db}\right]\right] \quad (1)$$

where A_g is the gross area of column, b is the overall width of section, d is the overall depth of section, and r is the radius of rounded corner.

Mirmiran et al. [10] proposed a logarithmic equation for a modified confinement ratio, MCR, to describe the behavior of square sections. The MCR is a function of corner radius, jacket size, and confining pressure describing the effectively confined area of concrete. Tests showed that when MCR $<15\%$, additional ductility is provided to the confined concrete, but there is no enhancement in strength. This means that when MCR $<15\%$ a square specimen with an FRP jacket would have an elastic–plastic or parabolic stress–strain curve showing little or no postpeak stiffness. The same jacket on a circular specimen would exhibit a bilinear stress–strain curve. It should be noted that for the work done by Mirmiran et al. [10], all FRP-confined cylinders exhibited bilinear stress–strain curves (high levels of confinement) while both bilinear and elastic–plastic behaviors were exhibited in FRP-confined circular specimens in this project.

Mirmiran et al. [10] also studied the effect of an adhesive or a mechanical bond between the FRP jacket and concrete specimen. No effect on load-carrying capacity was seen in comparing bonded specimens to unbonded specimens. A mechanical bond (shear connector) did improve the performance by distributing confinement pressures around the circumference of the FRP jacket tube.

3. Experimental program

The objective of this study is to refine the understanding of factors affecting the behavior of confined concrete. In this study, the effect of bonding the FRP jacket to the concrete substrate is investigated. It is proposed that by ensuring no bond and providing a small gap between the FRP jacket and the concrete cylinder, the contribution of the strain localization factor to the overall in situ jacket efficiency may be investigated.

Additionally, the shape factor is investigated. In this study, circular and square specimens are tested. The square specimens have their corners rounded to two different radii in an effort to experimentally validate an existing shape effect modification factor given by Eq. (1).

A series of 152-mm-diameter by 305-mm-tall concrete cylinders were tested [11] using standard test methods [12]. Variable passive confinement was provided by jacketing the cylinders in a lightweight E-glass material. The jackets were applied leaving a gap at the top and bottom of the cylinders to ensure that the jackets were not directly subject to axial load. The amount to confinement available (stiffness of jacket) was controlled by the number of plies used to wrap the cylinders. In this study, only 3 and 9 plies of E-glass material were used, representing low and moderately high levels of confinement, respectively [1]. Although the previous study and this study used different concrete batches, the results may be compared to ensure repeatability of results by normalizing by concrete strength. This comparison is presented later.

Cylinder specimens were provided with either bonded or unbonded jackets. The bonded jackets were applied in the traditional manner with an epoxy primer followed by the wet lay-up of an epoxy-based E-glass FRP fabric. For the unbonded cylinders, the surface primer was not applied. Instead, the cylinders were wrapped with two layers of a typical kitchen-type plastic wrap. Care was taken to keep the wrap smooth. The plastic wrap provides a gap of compressible material having a thickness of approximately 0.08 mm and prevents the FRP jacket from bonding to the concrete. This method of debonding was quite successful. It was possible to manually twist a cured FRP jacket around an unbonded cylinder.

An additional series of 152-mm-wide by 305-mm-tall square specimens were prepared with two different corner radii, r. A "small" corner radius of approximately $r=11$ mm was formed by applying a bead of silicon caulk in the corners of each form and smoothing with a finger. A "large" corner radius of $r=25$ mm was formed by placing quartered 51-mm-diameter PVC pipe in the corners of each form.

Table 1 provides jacket material properties for the raw material (manufacturer's data) and for tensile coupons tested as part of this study. The E-glass material exhibited a linear response to a sudden rupture failure. Coupon tests corresponding to all tested jacket stiffnesses (plies) were performed, the average values are reported in Table 1. The FRP

Table 1
FRP jacket material properties and test matrix

Parameter	Manufacturer's reported data	Experimentally determined data
Areal weight (g/m^2)	117	n.a.
Strength, $\bar{f}_{\text{fr}}$ (N/mm·ply)	154	75
Tensile modulus, $\bar{E}_{\text{f}}$ (kN/mm·ply)	10.3	4.9
Strain at rupture, ε_{fr}	0.015	0.016

Table 2
Summary of average experimental results for cylinders

Plies, n	0	0 [1]	3			9		
Bonded	n.a.	n.a.	Bonded	Bonded [1]	Unbonded	Bonded	Bonded [1]	Unbonded
f_{cmax} (MPa)	$f'_c = 31.8$	$f'_c = 32.1$	37.3	36.6	33.6	53.2	46.7	48.4
f_{cmax}/f'_c	1.00	1.00	1.17	1.14	1.06	1.68	1.46	1.52
ε_{tmax}	$\varepsilon'_t = 0.0019$	$\varepsilon'_t = 0.0017$	0.0032	0.0013	0.0054	0.0169	0.0111	0.0159
$\varepsilon_{tmax}/\varepsilon'_t$	1.00	1.00	1.69	0.77	2.87	9.00	6.39	8.46
ε_{cu}	0.0029	0.0039	0.0065	0.0050	0.0022	0.0095	0.0068	0.0022
ε_{tu}	0.0058	0.0091	0.0143	0.0120	0.0134	0.0169	0.0111	0.0178
FRP jacket strains (microstrain)								
Average ε_{jmax}	n.a.	n.a.	2585	2750	5314	14,383	11,321	12,848
S.D. ε_{jmax}			863	1559	800	1410	1260	822
Average ε_{ju}			12,155	9223	12,869	14,383	11,321	14,094
S.D. ε_{ju}			2469	3992	1519	1410	1260	910

coupon strength and stiffness were approximately 48% of the reported raw material properties.

4. Test apparatus and instrumentation

All specimens were tested in uniaxial compression [12] in a 2225-kN-capacity concrete cylinder test machine. Instrumentation recorded the applied axial load, axial and transverse strains, and strains on the FRP material itself. At least five specimens of each type were tested.

All confined specimens had electrical resistance strain gauges located at mid-height, oriented perpendicular to the longitudinal axis of the cylinder to measure hoop strain in the jackets. Eight strain gauges, spaced equidistant from each other around the circumference, were placed on the bonded and unbonded cylinders. Six strain gauges were also placed at the mid-height of the jacketed square specimens. Five of the gauges were placed around a corner in order to observe any difference in jacket strain as the jacket wrapped around the corner of the specimen. A sixth strain gauge was placed on one of the three remaining corners of the specimen.

A standard compressometer–extensometer was used to measure the axial and the transverse deformation of the cylinder [12]. The compressometer–extensometer was not used with the square specimens because it would not fit around the specimens. Instead, lateral and axial deformations were recorded with linear position sensors that were attached to the test frame. Values obtained from these instruments where used in determining the modulus and dilation parameters of the specimens.

5. Experimental results

Tables 2 and 3 give average values of the major parameters measured for the cylinders and square specimens, respectively. The values presented are averaged over at least five specimens. Fig. 3 shows representative axial stress versus strain curves for all the specimens types tested. For clarity, only one curve from each specimen type is shown and the horizontal axis for the square specimens has been shifted to the right.

5.1. Cylinder specimens

As indicated in Table 2, the results from this test series is comparable to data presented previously [1] for 3- and 9-ply

Table 3
Summary of average experimental results for square specimens

Plies, n	0		3		9	
Corner radius (mm)	25 (L)	11 (S)	25 (L)	11 (S)	25 (L)	11 (S)
f_{cmax} (MPa)	$f'_{cL} = 32.4$	$f'_{cS} = 31.2$	37.9	37.4	43.2	39.0
f_{cmax}/f'_c	1.00	1.00	1.17	1.20	1.33	1.25
ε_{cmax}	$\varepsilon'_{cL} = 0.0027$	$\varepsilon'_{cS} = 0.0016$	0.0018	0.0026	0.0046	0.0033
$\varepsilon_{cmax}/\varepsilon'_c$	1.00	1.00	0.68	1.64	1.70	2.07
ε_{cu}	0.0063	0.0027	0.0034	0.0063	0.0109	0.0125
$\varepsilon_{tu\ side}/\varepsilon_{tu\ corner}$	4.69	4.30	3.94	5.25	4.00	5.81
Effect of corner radius						
$A_{confined}$ from Eq. (1) (mm)	n.a.		15,955	11,870	15,955	11,870
$A_{confined\ L}/A_{confined\ S}$			1.34		1.34	
$f_{cmax\ L}/f_{cmax\ S}$	1.04		1.01		1.06	
$\varepsilon_{cmax\ L}/\varepsilon_{cmax\ S}$	1.69		0.69		1.39	

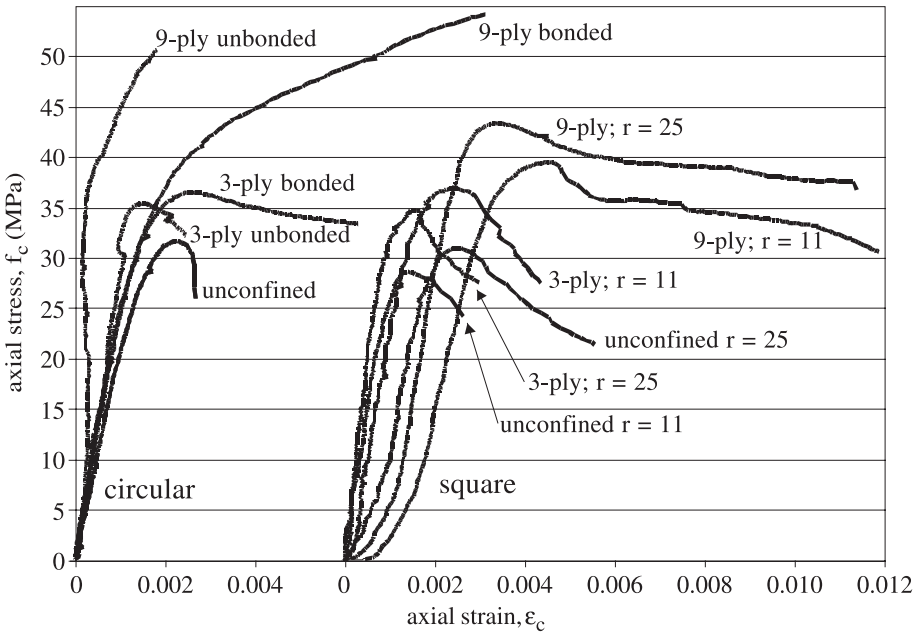

Fig. 3. Representative axial stress–strain behavior of tested specimens.

confined cylinders. FRP jacket strains, as recorded by the strain gauges around the jackets, were averaged and are also reported in Table 2 along with the standard deviation of the jacket strains around the jackets.

Stresses and strains were normalized using test results from the unconfined specimens. This allows for comparison with data from other tests [1]. The average unconfined compressive strength was 31.8 MPa and the corresponding axial strain was 0.0024 mm/mm. The symbols f_c' and ε_c' are used for these values, respectively.

Fig. 4 compares the transverse strain in the unbonded and bonded cylinders at strain levels less than f_c'. Fig. 5 shows the circumferential strain distributions around representative FRP jackets at various stress levels and at the eventual rupture of the jackets.

From Fig. 3, especially the 9-ply unbonded curve, it can be seen that axial strain data for the unbonded cylinders may not be reliable. This is probably due to the test set-up. Strain measurements are taken from the jacket, but when the jacket is not bonded to the concrete, the concrete cylinder can

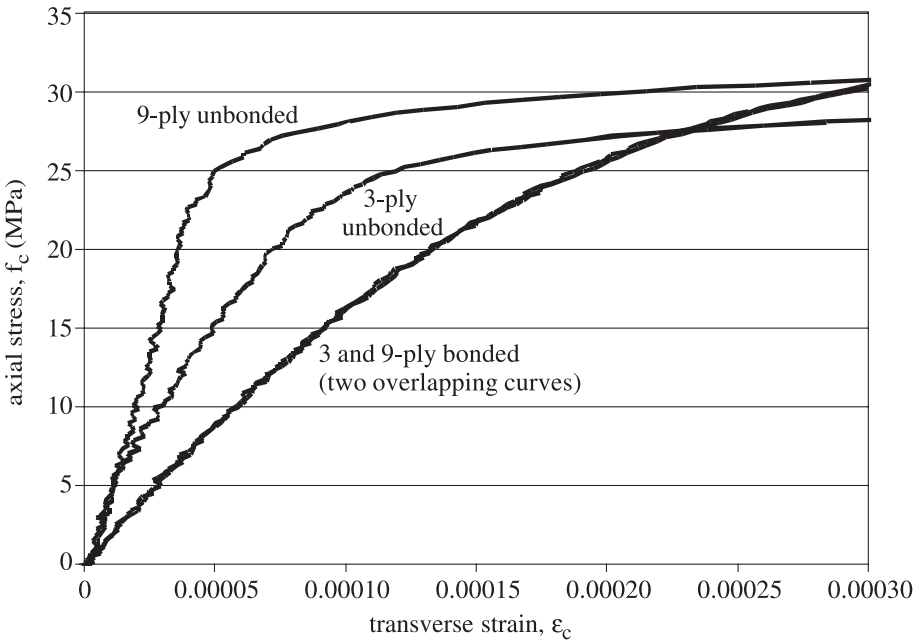

Fig. 4. Representative axial stress versus transverse strain curves illustrating gap closure.

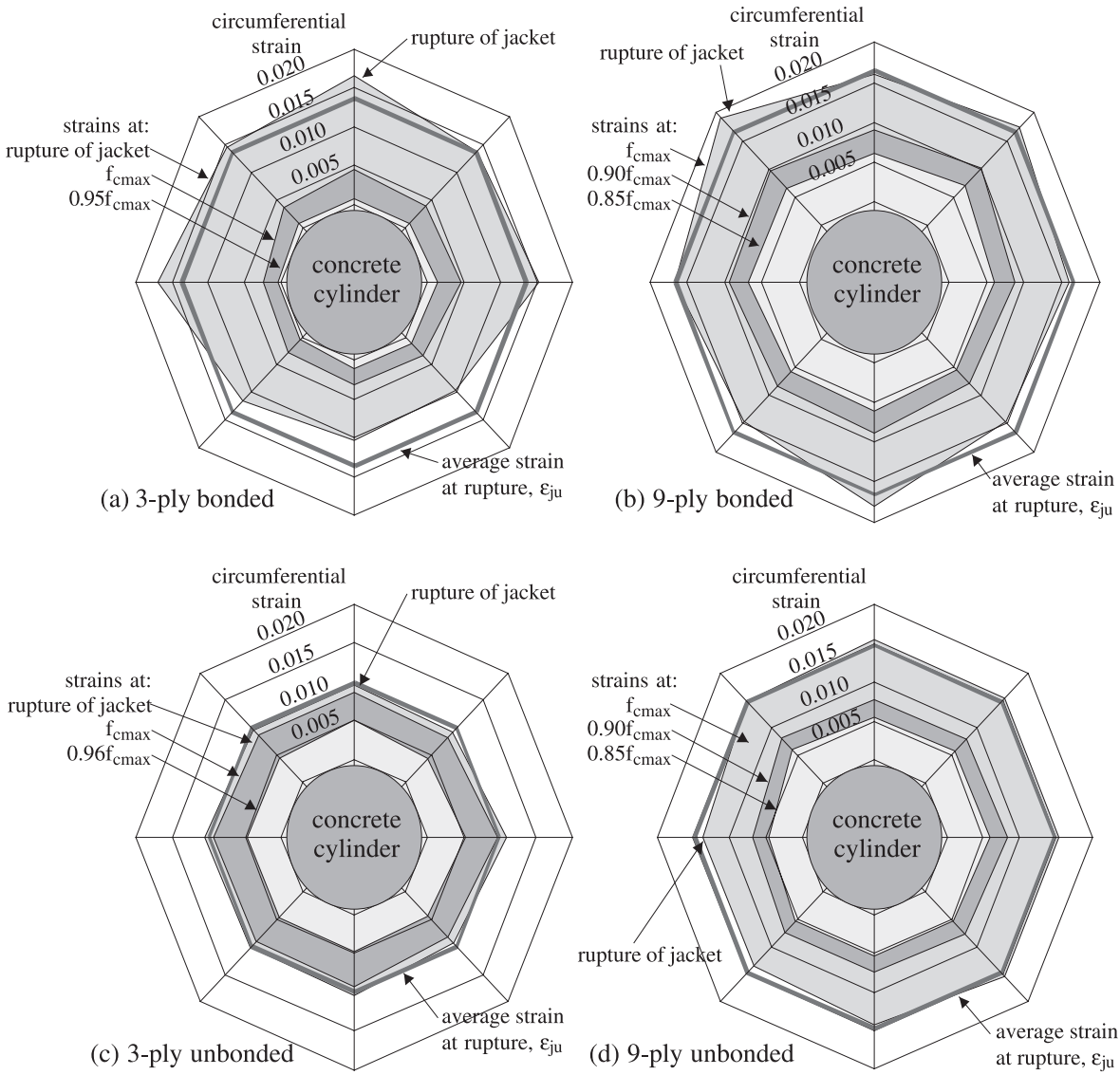

Fig. 5. Circumferential distribution of strain in FRP confining jackets.

move inside the jacket. As a result, accurate strain measurements from the compressometer–extensometer are not possible.

5.2. Square specimens

The unconfined compressive strength at the time of testing the square specimens was 32.4 MPa for the large-radius (25 mm) specimens and 31.2 MPa for the small-radius (11 mm) specimens. The corresponding axial strains were 0.0027 and 0.0016 mm/mm, respectively. As with the circular specimens, these values were defined as f'_c and ε'_c and used to normalize the data from the square-confined specimens.

The effective area of confined concrete was calculated using Eq. (1). The effective area of confined concrete, $A_{confined}$, for the large radius cylinders is 15,955 mm^2. The effective area of confined concrete, $A_{confined}$, for small radius cylinders is 11,870 mm^2. These values correspond to 70% and 51% of the gross section areas, respectively.

6. Discussions

6.1. Cylinder specimens

All cylinders exhibited stress–strain responses as expected. As shown in Fig. 3, the cylinders confined with 3 plies of E-glass material behaved as moderately confined cylinders having significant post peak ductility. The cylinders confined with 9 plies behaved as heavily confined cylinders having an essentially bilinear stress–strain response. This mirrors the behavior of cylinders tested previously [1]. The maximum confined concrete strength, f_{cmax}, is lower in the

unbonded cylinders. This was to be expected as the concrete in the unbonded cylinders must initially dilate to close the gap and engage the FRP jacket.

The gap in the unbonded cylinders appeared to close at an axial stress in the concrete of approximately 4000 psi or 85% of f'_c. At this point, the concrete dilation engages the FRP jacket. The size of the gap would influence at what percentage of f'_c the gap closes. A larger gap would close at a higher percentage of f'_c, while a smaller gap would close at a lower percentage of f'_c. Fig. 4 captures the gap closure. As expected, there is little initial jacket expansion in the unbonded cylinders at first. This is due to the cylinder expanding inside the jacket without engaging the instrumented jacket. After the gap closes, the transverse strain increases in the jacket as it begins to expand with the concrete. Due to the initially high concrete stress achieved in an effectively unconfined state (as the gap closes), the confining pressure at any given instant is a lower proportion of the axial stress than in a bonded specimen. Thus, the increase in load-carrying capacity brought about by confinement is reduced.

The gap did not affect the overall efficiency of the FRP jacket. The average ultimate strain in the unbonded cylinders is not significantly different from the average ultimate strain in the bonded cylinders. The strain distribution was slightly more uniform in the unbonded cylinders, as illustrated by comparing the standard deviation of the strains, but not to a significant degree as seen in Table 2 and Fig. 5.

Making column specimens in the laboratory with gaps between the concrete and FRP jacket may more closely model field conditions where columns are already under axial load when a jacket is applied. The initial column axial strain and dilation could be accurately modeled in the lab by applying an FRP jacket with a specified gap. The existing strains can be reached without confining pressure being engaged as the gap closes. Clearly, such a modeling technique would require an accurate measurement of the applied gap and a thorough understanding of the dilation response of the columns under investigation.

6.1.1. In situ strain efficiency factor, $\kappa_{\varepsilon 2}$

It was possible to manually rotate the unbonded jackets around the cylinders. Based on this, it is felt that the unbonded specimens accurately represent the case illustrated in Fig. 1(a) where $\kappa_{\varepsilon 1}$ is unity. The FRP rupture strains, ε_{ju}, observed in the unbonded cylinders (Table 2) are 86% and 94% of the manufacturer's reported rupture strain for the FRP material, ε_{fr}, for the 3- and 9-ply specimens, respectively. These ratios are somewhat higher than those observed elsewhere [3–5]. These higher values of $\kappa_{\varepsilon 2}$ may be attributable to the exceptional quality control achieved using the lightweight E-glass FRP used in this study, the smooth, form-cast sides of the cylinders, and the relatively small size of the specimens tested.

It is noted that, as indicated in Table 1, the value of ε_{fr} obtained from coupon tests was slightly greater than the manufacturer's reported value, resulting in values of $\kappa_{\varepsilon 2}$ of 0.80 and 0.88 for the 3- and 9-ply specimens, respectively.

6.1.2. Strain localization factor, $\kappa_{\varepsilon 1}$

Comparing the average jacket strains at rupture, ε_{ju}, to the maximum jacket strain observed, ε_{jr}, for the bonded specimens, as shown in Fig. 5(a) and (b), one can arrive at an estimate of the strain localization factor, $\kappa_{\varepsilon 1}$. Based on experimental results, the value of $\kappa_{\varepsilon 1}$, expressed as the ratio $\varepsilon_{ju}/\varepsilon_{jr}$, ranges from 0.75 to 0.90. This value is approximately 0.82 and 0.86 for the representative 3- and 9-ply specimens shown in Fig. 5(a) and (b), respectively.

Typically, the experimentally observed value of ε_{jr} is greater than the manufacturer's reported rupture strain for the material, ε_{fr}. To obtain a normalized value of $\kappa_{\varepsilon 1}$, the ratio $\varepsilon_{ju}/\varepsilon_{fr}$ is considered. For the bonded specimens tested, this value is 0.81 and 0.96 for the 3- and 9-ply jackets, respectively.

6.1.3. Strain efficiency factor, κ_{ε}

Thus, for the high quality, small-scale specimens tested, the total strain efficiency factor, κ_{ε}, given as the product of the strain localization factor, $\kappa_{\varepsilon 1}$, and the in situ properties factor, $\kappa_{\varepsilon 2}$, was found to be 0.70 and 0.90 for the 3- and 9-ply specimens, respectively. These values are somewhat greater than reported elsewhere [3–5] although Kestner et al. [3] does also report similar higher values for similar sized specimens. Significantly, this result suggests that the strain efficiency factor is additionally affected by the level of confinement provided.

6.2. Square specimens

Similar to the circular specimens, the maximum confined concrete stress and strain are observed to increase with increasing confinement. This increase, however, is significantly less for the square section shape. For the specimens tested, it can be said that the 9-ply jacketed square sections exhibited moderate levels of confinement while the 3-ply exhibited behavior typical of low levels of confinement [1].

An expected increase in strain at the corners of the jackets, where confining pressure is generated, was not observed. The corners of the FRP jacket are in tension while the jacket along the flat sides of the specimen behaves primarily in flexure as the concrete section dilates. Because the jacket thickness is small, the tensile strains associated with flexure are far in excess of those associated with the confining tension or hoop stress. Thus, surface-mounted strain readings are inappropriate for determining effective confining pressure in noncircular shapes. The ratio of observed jacket strains along the sides of the section to those at the corners at failure of the jacket is approximately 4.5 as indicated in Table 3. Finally, because the jacket is bonded to the concrete, there arises a discontinuity at the beginning of the radius as the side of the section transitions into the quarter-circular corner. In all cases, the FRP jackets

Table 4
Effective area of confined concrete

Shape	Corner radius (mm)	Plies, n	f_{cmax} (MPa) calculated using		$A_{confined}/A_g$	$(f_{cmax}(A_{confined}))_{circular}/(f_{cmax}(A_{confined}))_{square}$
			A_g (Table 3)	$A_{confined}$ (Eq. (1))		
Circular	n.a.	3	37.3		1.00	1.00
		9	53.2			
Square	11	3	37.4	72.8	0.51	0.51
		9	39.0	76.0		0.70
Square	25	3	37.9	53.9	0.70	0.69
		9	43.3	61.4		0.87

were observed to rupture at this location. Accounting for the flexure-induced strains and the discontinuity, the strain efficiency of the square jackets is significantly reduced from that of the circular jackets.

It is concluded that Eq. (1) cannot be used to draw a comparison between different radii and maximum strength. Eq. (1) does not consider the size of the jacket. Although the flexural strength of the FRP jacket is small in comparison to its tensile strength, a 3-ply jacket may have a different effective area of confined concrete compared to a 9-ply jacket due to the difference in jacket thickness. As seen from Table 3, the strength and axial strain ratios from the two radii increased as the jacket size increased. This increase, however, was not proportional to the increase in the proposed effectively confined area.

Table 4 compares the axial stress in the square specimens determined based on the assumed equivalent area of confined concrete (Eq. (1)) to the axial stress in the circular specimens having the same confining jackets. The axial stress calculated based on an effective confined area should be approximately equal to stress in the circular specimens subject to the same confinement. For the cases tested, the ratio $(f_{cmax}(A_{confined}))_{circular}/(f_{cmax}(A_{confined}))_{square}$ is less than unity, indicating that Eq. (1) is underestimating the effectively confined area. This underestimation is partially a function of not accounting for the residual stresses carried in the unconfined region of the section. However, this does not account for all of the underestimation. It is suggested that Eq. (1) may not be appropriate for the scale of the specimens tested here but may yield better predictions of equivalent confinement for larger specimens where the ratio $A_{confined}/A_g$ is greater. Further investigation is required to investigate this.

7. Summary and conclusions

The effect of several parameters on the axial stress–strain behavior of concrete confined with FRP jackets has been presented. These parameters include jacket bond to concrete surface and cross section shape. The following conclusions can be made from the experimental results obtained in this study:

1. The confined concrete cylinders behaved like similar specimens tested in a previous study [1]. Both test series resulted in moderately confined concrete behavior when a 3-ply jacket was used and heavily confined concrete behavior when a 9-ply jacket was used.
2. Maximum concrete strength, f_{cmax}, is lower in concrete confined with unbonded FRP jackets.
3. The gap in the unbonded cylinders tested closed at an axial stress in the concrete of approximately 4000 psi or 85% of f'_c. The provision of the gap did not significantly affect the overall efficiency of the FRP jacket.
4. Experimentally determined values of the in situ properties factor, $\kappa_{\varepsilon 2}$, are approximately 0.90. These values vary considerably and are higher than those reported elsewhere although reasons for this improved behavior are proposed.
5. Experimentally determined values of the strain localization factor, $\kappa_{\varepsilon 1}$, range from 0.75 to 0.90.
6. The total strain efficiency factor, κ_{ε}, appears to be additionally affected by the level of confinement provided.
7. The shape of the column affects the level of confinement generated. Square columns exhibit lower confinement levels than do circular columns with the same jacket.
8. A previously proposed relationship (Eq. (1)) for the area of effectively confined concrete in a rectilinear section [8] does not appear to capture the effect of square columns having different corner radii. This relationship appears to underestimate the effectively confined area for the specimens tested.

8. Further research

Through the course of this research, the following have been identified as the areas for further investigation.

1. Further research is needed to better understand the influence of a gap between the FRP jacket and concrete surface. It is believed that the unbonded cylinders exhibited lower strength because of the initial dilation of the cylinder required to engage the jacket. Further research needs to be done to verify this. Examining different gap sizes in future research may lead to practical experimental applications where a gap may be used to model existing stresses (or strains) in a jacketed column.
2. The effect of confinement on larger scale specimens and those having internal reinforcement is required to verify

that large-scale specimens perform in a similar manner as small-scale specimens.

3. Further parametric study is required to develop empirical relationships for the strain efficiency factors. Results of this study have indicated that, in addition to previously identified factors, specimen scale, and level of confinement appear to affect the efficiency of the jacket.
4. Due to bulging of the FRP jacket, the tensile stresses in the square FRP jacket do not correlate directly with confinement provided. Further parametric investigation is required to accurately determine the level of confinement provided by rectilinear jackets.

Notation used

$A_{confined}$	effective area of confined concrete
A_g	gross area of concrete section
b	overall width of section
d	overall depth of section (for square specimens $b=d$)
$\bar{E}_f$	tensile modulus of FRP material
$\bar{f}_{fr}$	strength of FRP material
f_{cmax}	maximum strength of confined concrete, for unconfined specimens $f_{cmax}=f'_c$
f'_c	unconfined concrete compressive strength
f_{con}	confining pressure
n	number of plies of FRP material
r	corner radius of rectilinear section
ε_{cmax}	strain in confined concrete corresponding to f_{cmax}, for unconfined concrete $\varepsilon_{cmax}=\varepsilon'_c$
ε_{cu}	ultimate axial strain of concrete (for heavily confined concrete $\varepsilon_{cu}=\varepsilon_{cmax}$)
ε'_c	concrete compressive strain corresponding to f'_c
ε_{fr}	rupture strain of FRP coupon
ε_{jr}	in situ rupture strain of FRP jacket
ε_{tmax}	transverse strain in confined concrete corresponding to f_{cmax}, for unconfined concrete $\varepsilon_{tmax}=\varepsilon'_t$
ε_{tu}	ultimate transverse strain of concrete (for heavily confined concrete $\varepsilon_{tu}=\varepsilon_{tmax}$)
ε'_t	concrete transverse strain corresponding to f'_c
κ_ε	strain efficiency factor
$\kappa_{\varepsilon 1}$	strain localization factor
$\kappa_{\varepsilon 2}$	in situ properties factor

Acknowledgements

This research was partially funded by a USC Research and Productive Scholarship Award. The authors would like to acknowledge the assistance of Ms. Gayatri Kharel. Composite Structures Technology is acknowledged for their assistance with the lightweight FRP materials.

References

[1] K.A. Harries, G. Kharel, Experimental behavior of variably confined concrete. Cem. Concr. Res. 33 (2003) 873–880.
[2] K.A. Harries, G. Kharel, Behavior of variably confined concrete, ACI Mater. J. 99 (2) (2002) 180–189.
[3] J. Kestner, K.A. Harries, S. Pessiki, R. Sause, J.M. Ricles, Rehabilitation of reinforced concrete columns using fiber reinforced polymer composite jackets, Lehigh University ATLSS Report No. 97-07, 1997, 196 pp.
[4] M. Demers, Détermination des Paramètres Influençant le Comportement des Collones en Béton Confinées par une Enveloppe Mince en Composite D'Avant-Garde, MASc Thesis, Université de Sherbrooke, 1994, 98 pp.
[5] G. Kharel, Behavior and modeling of variably confined concrete, MSc Thesis, Department of Civil and Environmental Engineering, University of South Carolina, 2001, 98 pp.
[6] S. Pessiki, K.A. Harries, J. Kestner, R. Sause, J.M. Ricles, The axial behavior of concrete confined with fiber reinforced composite jackets, ASCE J. Compos. Constr. 5 (4) (2001) 237–245.
[7] ASTM D3039-00, Standard Test Method for Tensile Properties of Polymer Matrix Composite Materials, ASTM, West Conshohocken, PA, 2000.
[8] J.I. Restrepol, B. DeVino, Enhancement of the axial load carrying capacity of reinforced concrete columns by means of fiberglass–epoxy jackets, Proc. Adv. Compos. Mater. Bridges Struct. II, Montreal (1995) 547–553.
[9] R. Park, T. Paulay, Reinforced Concrete Structures, Wiley, New York, 1975.
[10] A. Mirmiran, M. Shahawy, M. Samaan, H.E. Echary, J.C. Mastrapa, O. Pico, Effect of column parameters on FRP-confined concrete, ASCE J. Compos. Constr. 2 (4) (1998) 175–185.
[11] S. Carey, Behavior of variably confined concrete, Honors College Thesis, Department of Civil and Environmental Engineering, University of South Carolina, 2002, 60 pp.
[12] ASTM C39-96, Standard Test Method for Compressive Strength of Cylindrical Concrete Specimens, ASTM, West Conshohocken, PA, 1996.